JOURNAL OF GEOPHYSICAL RESEARCH, VOL. 97, NO. A7, PAGES 10,825–10,830, JULY 1, 1992

Energy Spectrum of Particles Accelerated Near a Magnetic x Line

D. L. BRUHWILER[1] AND ELLEN G. ZWEIBEL

Department of Astrophysical, Planetary, and Atmospheric Sciences
University of Colorado, Boulder

We study the acceleration of test particles near a static magnetic x line with a uniform electric field and a strong component of the magnetic field, $B_\parallel$, parallel to the x line. The energy spectrum of the accelerated particles is found analytically in the nonrelativistic limit, showing good agreement with numerical simulations. At high energies, the spectrum decays exponentially with a characteristic energy very different from that found in studies assuming $B_\parallel = 0$.

INTRODUCTION

It is generally accepted that solar flares involve the rapid release of energy stored in the coronal magnetic field and that magnetic reconnection is the most likely mechanism by which energy is released [*Sturrock*, 1980]. Solar flares are characterized by the rapid (on time scales as short as tens of milliseconds) onset of hard X ray emission. This emission, together with the γ ray line emission that often appears, suggests that electrons and ions are rapidly accelerated to energies hundreds of times greater than their preflare energy.

A number of acceleration mechanisms for solar flare particles have been proposed [*Forman et al.*, 1986]. In this paper we explore one of these: acceleration by the electric field which accompanies magnetic reconnection. Previous workers have modeled reconnection regions as a static x line [e.g., *Parker*, 1957; *Sweet*, 1958; *Petschek*, 1964; *Syrovatskii*, 1966; *Friedman*, 1969; *Martin*, 1986; *Burkhart et al.*, 1990]. The most important new feature of our work is that we allow a third vector component of the magnetic field; i.e., the field is sheared and the x line appears only in projection.

Bulanov and Syrovatskii [1976] obtained approximate analytic expressions for the motion of test particles near a static, two-dimensional magnetic x line with a uniform electric field directed parallel to the x line. They considered only those particles so close to the neutral line that the electric field played a dominant role. *Bulanov and Sasorov* [1976] then used these results to obtain asymptotically the exponentially decaying high-energy tail of the accelerated distribution. Their work largely explained the earlier numerical results of *Friedman* [1969]. Later, *Martin* [1986] showed that the dynamics in this system is chaotic when the electric field is small, but his findings are not inconsistent with the results of Bulanov and Syrovatskii.

We consider the effect of adding to Bulanov and Syrovatskii's model a magnetic field component parallel to the x line, $B_\parallel$. In order to facilitate an analytic approach, we assume $B_\parallel$ to be large compared with the perpendicular components. Such a geometry is likely to occur if the acceleration takes place in or along coronal flux tubes [*Chiueh and Zweibel*, 1987].

We approximately solve the equations of motion in this new field configuration. Then, starting with a thermal initial distribution, we use these results to calculate final velocity and energy spectra for the accelerated distribution. Like *Bulanov and Sasorov* [1976], we find that the energy distribution has an exponential tail. However, the scaling of the e-folding energy with the various parameters in the problem is very different in our case than in theirs.

It is worth emphasizing that the addition of a strong parallel magnetic field component results in adiabatic motion, at least over relevant time scales and within the domain of interest. To lowest order, particles are simply accelerated along the field lines, and drifts are unimportant. Thus the chaos associated with the $B_\parallel = 0$ case has essentially been removed.

MODEL

We consider the expansion of a static magnetic field $\mathbf{B}$ near an x line, assuming that the dominant component $B_\parallel$ lies along the x line. The field geometry is three dimensional with the x line defining the z axis, but $\mathbf{B}(x, y)$ is taken to be independent of z. We also suppose a static, uniform electric field oriented along the x line. The fields are given by the following:

$$\mathbf{B}(x, y) = B_0 \frac{y}{D}\mathbf{x} + a^2 B_0 \frac{x}{D}\mathbf{y} - B_\parallel \mathbf{z}; \qquad (1a)$$

$$\mathbf{E} = E_\parallel \mathbf{z}. \qquad (1b)$$

We take B_0, $B_\parallel$, and $E_\parallel$ to be positive. The projection of the magnetic fieldlines onto the x-y plane is shown in Figure 1. Equations (1a) and (1b) are only expected to hold for $a|x|$, $|y| \le D$, where $a \equiv \tan\psi \le 1$, ψ is the angle between the x axis and the separatrix, and D is the characteristic length scale over which one can make a local expansion of $\mathbf{B}$ about its x line. The use of D is of course artificial and is only meant to crudely model the physical system. The assumption that $\mathbf{B}$ and $\mathbf{E}$ are

[1]Currently at Grumman Space Systems, Princeton, New Jersey.

Copyright 1992 by the American Geophysical Union.

Paper number 92JA00828.
0148-0227/92/92JA-00828$05.00

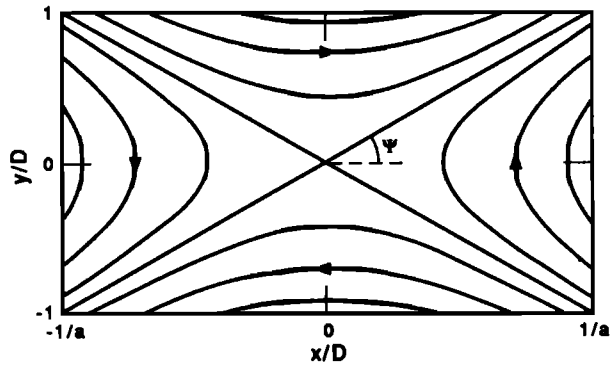

Fig. 1. Projection of magnetic field lines onto x-y plane; $\psi = \tan^{-1}(a)$.

static is reasonable provided that the acceleration time is short compared to the time scale over which the fields evolve. We check this assumption a posteriori.

The nonrelativistic Lorentz force implies the following equations of motion for a test particle:

$$\ddot{x} = -\Omega_{\|}\dot{y} - a^2\Omega_0\frac{x}{D}\dot{z}; \tag{2a}$$

$$\ddot{y} = \Omega_{\|}\dot{x} + \Omega_0\frac{y}{D}\dot{z}; \tag{2b}$$

$$\ddot{z} = \frac{e}{m}E_{\|} + a^2\Omega_0\frac{x}{D}\dot{x} - \Omega_0\frac{y}{d}\dot{y}. \tag{2c}$$

The gyrofrequency of particles near the x line is $\Omega_{\|} \equiv eB_{\|}/mc$, where e and m are the particle electric charge and mass, respectively, and c is the speed of light. Similarly, $\Omega_0 \equiv eB_0/mc$.

We can nondimensionalize equations (2a)–(2c) by using $1/\Omega_{\|}$ as the unit of time and D as the unit of distance. We also define the small parameter $\epsilon \equiv \Omega_0/\Omega_{\|}$ and a dimensionless electric field E_0, given by $\epsilon E_0 \equiv eE_{\|}/mD\Omega_{\|}^2$. Furthermore, equation (2c) can be integrated once to obtain $\dot{z}$ as a function of x, y, and t. This result can then be inserted into equations (2a) and (2b), yielding

$$\ddot{x} + \dot{y} = -\epsilon a^2 x\,(\dot{z}_0 + E_0\epsilon t) - \epsilon^2 a^2 x\frac{1}{2}\left[\left(a^2x^2 - y^2\right) - \left(a^2x_0^2 - y_0^2\right)\right]; \tag{3a}$$

$$\ddot{y} + \dot{x} = \epsilon y\,(\dot{z}_0 + E_0\epsilon t) + \epsilon^2 y\frac{1}{2}\left[\left(a^2x^2 - y^2\right) - \left(a^2x_0^2 - y_0^2\right)\right]. \tag{3b}$$

Here x_0, y_0, and $\dot{z}_0$ are the initial values, respectively, of x, y, and $\dot{z}$, and the initial value of t is taken to be zero. Clearly, there will be some sign changes in equations (3) if the electric charge e is negative (i.e., if the particle is an electron), but these changes do not affect the dynamics in any significant way.

Equations (3a) and (3b) can be solved approximately in a number of different limits, depending on the values of the various parameters. We now delimit these parameters to the extent possible. For example, the smallness of ϵ depends on how loosely **B** winds around the coronal loop(s); we will assume that $\epsilon \lesssim 0.1$ and treat it as being small. The parameter a^2 can be very small or of order unity, depending on one's chosen model; we do not make any assumptions about its magnitude. Because of our chosen nondimensionalization, the initial conditions (ax_0, y_0) and the variables (ax, y) are all of order unity.

In Table 1, we present order of magnitude numbers for the range of certain physical parameters in the solar corona during a flare. These numbers are to be used only as rough guides, so we do not try to justify them. The characteristic distance D ranges so widely because it is not readily constrained by reconnection models. The lower limit comes from a Petschek model, using the classical conductivity of the coronal plasma [*Friedman*, 1969]; this number could increase by orders of magnitude if an anomalous or turbulent resistivity were used. The upper limit on D comes from estimates of the scale over which coronal magnetic fields change [*Van Hoven*, 1976], and a similar number emerges in Syrovatskii's paper on the "dynamic dissipation" of a current sheet [*Syrovatskii*, 1966].

TABLE 1. Rough Physical Parameters for Flares

Physical Parameter	Lower Limit	Upper Limit
Density, n (cm^{-3})	1×10^9	2×10^{11}
B field, $B_{\|}$ (G)	100	500
Temperature, k_BT (eV)	50	500
Distance, D (cm)	10	1×10^6

Even given these numbers for the relevant physical parameters, it is impossible to delimit E_0 without specifying the physical mechanism which produces $E_{\|}$. To be explicit, we assume that the electric field arises inductively, because of plasma flow across the field lines, (i.e., toward the x line along the y axis and away from the x line along the x axis), and parameterize it by an inflow velocity V: $E_{\|} \sim VB_0/c$. It is because of this assumption that an ϵ appears explicitly in front of E_0.

If we further assume that $V \sim \mu v_{A0}$, where v_{A0} is the Alfvén speed for B_0 and μ is a dimensionless parameter, then $E_0 \sim (1 \times 10^4)\epsilon\mu(m/m_e)/D[\mathrm{cm}]n^{1/2}[\mathrm{cm}^{-3}]$, where m_e is the electron mass. The resulting (order of magnitude) range in values for $E_0/\epsilon\mu$ is given in Table 2. Table 2 also shows the range of values for r_g, which is defined to be the gyroradius of a thermal particle in our dimensionless units: $r_g \equiv v_{th}/D\Omega_{\|} \sim 2(m/m_e)^{1/2}(k_BT)^{1/2}[\mathrm{ev}]/D[\mathrm{cm}]B_{\|}[\mathrm{gauss}]$.

TABLE 2. Approximate Range of Nondimensional Parameters E_0 and r_g

Parameter	Particle	Lower Limit	Upper Limit
$E_0/\epsilon\mu$	ions	6×10^{-5}	100
$E_0/\epsilon\mu$	electrons	3×10^{-8}	5×10^{-2}
r_g	ions	1×10^6	2
r_g	electrons	2.5×10^{-8}	5×10^{-2}

Approximate range as per information in Table 1 and model-dependent assumptions made in the text.

RESULTS

Our goal is to understand the particle dynamics well enough to predict the final distribution of accelerated particles. Since our fields are just a local expansion about the x line, we cannot know what happens to them once they leave the "box" shown in Figure 1, so we simply assume that they stop being accelerated at that point. During the time that a particle is in the box, it is accelerated in the z direction according to the equation

$$\dot{z}(t) = \dot{z}_0 + E_0\epsilon t + \epsilon\frac{1}{2}\left[\left(a^2x^2 - y^2\right) - \left(a^2x_i^2 - y_i^2\right)\right], \quad (4)$$

where (x_i, y_i) is the initial guiding center position. Equation (4) is obtained by integrating equation (2c) and nondimensionalizing. To obtain a final velocity, we only need to know how long each particle remains near the x line.

According to Table 2, the gyroradius is very small in most cases (in all cases for electrons), so guiding center theory should be applicable [*Nicholson*, 1983]. Guiding center theory also assumes that the component of $\mathbf{E}$ parallel to $\mathbf{B}$ is of the order of the gyroradius (i.e., small). Here $\mathbf{E}$ is independent of the gyroradius, but the dimensionless electric field ϵE_0 is of the order of ϵ and hence is small. Because $B_\parallel$ does not vanish at the x line, guiding center theory remains valid even in the vicinity of the x line. Rather than trying to solve the problem by using guiding center coordinates, however, we consider in turn free-streaming motion along magnetic field lines, then the $\mathbf{E}\times\mathbf{B}$ drift, the grad-B drift, and the curvature drift, ultimately showing that drifts can be ignored for typical particles. We then obtain an approximate solution for the x-y motion by ignoring drifts and use this result to calculate the parallel velocity spectrum attained by an initial ensemble.

To lowest order, particles stream along the magnetic field lines, with a velocity $\dot{z} \sim \epsilon E_0 t$, moving a distance $\Delta z \sim \epsilon E_0 t^2/2$. In order to leave the box, such particles must traverse a distance $1/a$ in the x-y plane, but the field lines are oriented primarily along the z axis, which means these particles must move a distance $\Delta z \sim 1/\epsilon a$ along the z axis. This implies a characteristic time scale for leaving the box:

$$\tau_{\text{stream}} \sim \epsilon^{-1}\left(E_0 a\right)^{-1/2}. \quad (5)$$

The $\mathbf{E}\times\mathbf{B}$ drift velocity is given by $\mathbf{v}_{\mathbf{E}\times\mathbf{B}} = c(\mathbf{E}\times\mathbf{B})/B^2$ [*Nicholson*, 1983]. In dimensionless units, $v_{\mathbf{E}\times\mathbf{B}} \sim \epsilon^2 E_0$, and the vector lies in the x-y plane. Thus particles will $\mathbf{E}\times\mathbf{B}$ drift a distance $1/a$ in a characteristic time $\tau_{\mathbf{E}\times\mathbf{B}}$, where

$$\tau_{\mathbf{E}\times\mathbf{B}} \sim \epsilon^{-2}\left(E_0 a\right)^{-1}. \quad (6a)$$

The ∇B drift velocity is given by [*Nicholson*, 1983]:

$$\mathbf{v}_{\nabla B} = v_\perp^2\left(\mathbf{B}\times\nabla B\right)/2B^2\Omega_\parallel$$

where $v_\perp = \left(v_x^2 + v_y^2\right)^{1/2}$ is roughly the thermal velocity and the vector $\nabla B \sim \epsilon B_0$ lies in the x-y plane. In dimensionless form, $v_{\nabla B} \sim \epsilon^2 r_g^2$, and it too lies in the x-y plane. Thus particles will ∇B drift a distance $1/a$ in a characteristic time $\tau_{\nabla B}$:

$$\tau_{\nabla B} \sim \left(\epsilon r_g\right)^{-2} a^{-1}. \quad (6b)$$

The curvature drift velocity is given by $\mathbf{v}_{\text{curve}} = v_\parallel^2\left(\mathbf{E}_B\times\partial_s E_B\right)/\Omega_\parallel$ [*Nicholson*, 1983], where $\mathbf{E}_B \equiv \mathbf{B}/B$ is a unit vector parallel to $\mathbf{B}$, and $\partial_s \equiv \mathbf{E}_B\cdot\nabla$ is the spatial derivative along a field line. To lowest order, $v_\parallel = \dot{z} \sim \epsilon E_0 t$, and $\partial_s \mathbf{E}_B \sim a^2\epsilon^2$. These results yield a dimensionless drift velocity $\mathbf{v}_{\text{curve}} \sim a^2\epsilon^4 E_0^2 t^2$, which lies in the x-y plane. Integrating $\mathbf{v}_{\text{curve}}$ yields a traversed distance $\Delta x \sim a^2\epsilon^4 E_0^2 t^3/3$, and setting this distance equal to $1/a$ yields a characteristic time scale τ_{curve}, where

$$\tau_{\text{curve}} \sim a^{-1}\left(\epsilon^4 E_0^2\right)^{-3}. \quad (6c)$$

Each of these four time scales can vary by orders of magnitude, but τ_{stream} is the shortest in the limit that $\epsilon << 1$, $a \lesssim 1$, and $r_g \lesssim E_0 < 1$. This means that drifts are a negligible correction to the motion of typical trajectories. We could proceed by solving the parallel equation of guiding center theory, $m dv_\parallel/dt = eE_\parallel$. However, this seemingly simple equation would have to be solved in guiding center coordinates (i.e., in a curvilinear coordinate system based on the local direction of $\mathbf{B}$), which would be awkward, because the field lines converge and diverge hyperbolically near the x line, resulting in a complicated topology. It is easier and more natural to approximately solve the full equations of motion in the Cartesian coordinate system.

We solve approximately for the free-streaming motion by using the method of multiple time scales [*Bender and Orszag*, 1978]. We define a slow time $\lambda \equiv \epsilon t$, which is an order-unity quantity. Both x and y are expanded as power series in ϵ, with each term taken to depend explicitly on both t and λ. Equations (3a) and (3b) then separate into a hierarchy of equations which can be solved order by order in ϵ, with the slow time behavior of the lower-order equations being obtained by requiring that secular terms in the higher-order equations vanish. Solving these equations to first order in ϵ, we find the following lowest-order result:

$$x_0(t,\lambda) = x_{\text{gc}}(\lambda) + r_g\cos\left[t + \phi(\lambda)\right]; \quad (7a)$$

$$y_0(t,\lambda) = y_{\text{gc}}(\lambda) + r_g\sin\left[t + \phi(\lambda)\right]. \quad (7b)$$

The gyroradius r_g is an adiabatic invariant: it changes only by an amount of order ϵ in a time interval of the order of $1/\epsilon$. The magnetic moment $\mu \sim r_g^2/|\mathbf{B}|$ is therefore also an adiabatic invariant, because $|\mathbf{B}|$ varies only by an amount of order ϵ^2 within the box.

The slow evolution of the guiding center position and the gyrophase are given by the following:

$$x_{\text{gc}}(\lambda) = x_i\cosh\left[a\left(\dot{z}_0\lambda + \frac{1}{2}E_0\lambda^2\right)\right] - \frac{1}{a}\,y_i\sinh\left[a\left(\dot{z}_0\lambda + \frac{1}{2}E_0\lambda^2\right)\right]; \quad (8a)$$

$$y_{\text{gc}}(\lambda) = y_i\cosh\left[a\left(\dot{z}_0\lambda + \frac{1}{2}E_0\lambda^2\right)\right] - a\,x_i\sinh\left[a\left(\dot{z}_0\lambda + \frac{1}{2}E_0\lambda^2\right)\right]; \quad (8b)$$

$$\phi(\lambda) = \phi_i - \frac{1}{2}\left(1 - a^2\right)\left(\dot{z}_0\lambda + \frac{1}{2}E_0\lambda^2\right). \quad (8c)$$

Equations (7) and (8) neglect order ϵ corrections to the motion, and they are valid for time intervals of the order of $1/\epsilon$ or less.

The x-y projections of some numerically integrated trajectories are shown in Figure 2. On the fast time scale t, particles gyrate around the z component of $\mathbf{B}$, with gyroradius r_g. On the slow time scale λ, they drift along the x-y projection of the magnetic field lines. This motion is consistent with our assumption that particles are streaming along the three-dimensional field lines. We note that a symplectic algorithm [*Channell and Scovel*, 1990] was used for all our numerical work. Nonsymplectic algorithms introduced spurious damping which qualitatively changed the motion.

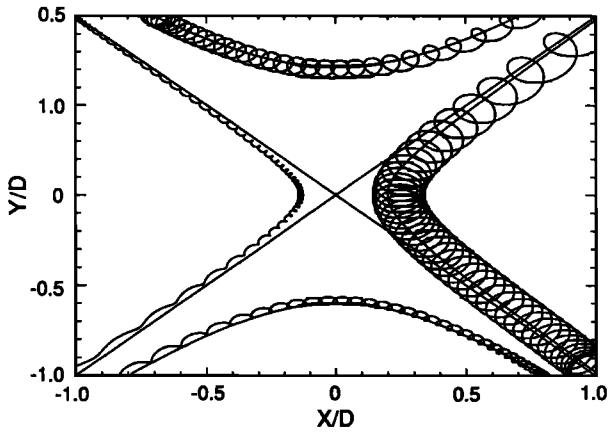

Fig. 2. Projection of particle trajectories onto x-y plane, for $\epsilon = 10^{-2}$, $a = 1$, $E_0 = 0.5$ and various values of r_g.

We now obtain the parallel velocity spectrum of an initially thermal ensemble by calculating how long a given particle will remain in the box. If we neglect thermal motions (i.e., $r_g, \dot{z} \to 0$), equations (8a) and (8b) can be explicitly inverted to obtain the time t_f at which a particle's guiding center leaves the box:

$$t_f = \frac{1}{\epsilon}\left(\frac{2}{aE_0}\ln\left[\frac{|y_i + ax_i|}{1 + \left(1 - \left|y_i^2 - a^2x_i^2\right|\right)^{1/2}}\right]\right)^{1/4}. \quad (9)$$

This can be checked by inserting equation (9) into equation (8a) or (8b), depending on the location of the initial position. We obtain the final parallel velocity by inserting equation (9) into equation (4), while neglecting $\dot{z}_0$ and the order ϵ term: $\dot{z}_f \approx E_0\epsilon t_f$.

Bulanov and Sasorov [1976] argue that, if particles are $\mathbf{E} \times \mathbf{B}$ drifting into the vicinity of the x line, then they should be uniformly distributed in position near the x line. We make the same assumption in order to compare our result with theirs. Given an initial ensemble uniformly distributed throughout our box, $f(\dot{z}_0, x_i, y_i) = \text{const}$, we can find the final velocity distribution by averaging the final ensemble, $f(\dot{z}_f, x_i, y_i) \equiv f(\dot{z}_0, x_i, y_i)d\dot{z}_f/d\dot{z}_0$, over x_i and y_i:

$$f(\dot{z}_f) = N_{\text{tot}}\frac{a}{E_0}\dot{z}_f\left[\cosh\left(a\dot{z}_f^2\right) + 1\right]^{-1}, \quad (10)$$

where N_{tot} is the total number of particles. We plot

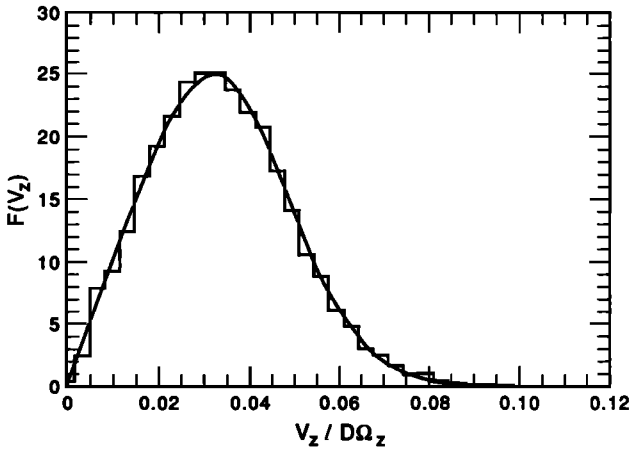

a

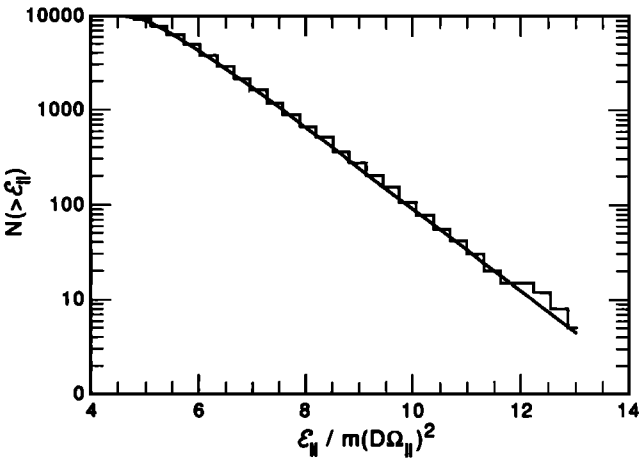

b

Fig. 3. (a) Analytical velocity spectrum $f(\dot{z}_f)$, for $\epsilon = 10^{-2}$, $a = 1$, $E_0 = 5 \times 10^{-4}$, and $r_g = 10^{-4}$, compared with a simulation involving 5×10^3 particles placed in 30 bins; (b) Exponential tail of the analytical energy spectrum $N(\mathcal{E}_\parallel)$, for $\epsilon = a = E_0 = 10^{-2}$ and $r_g = 10^{-4}$, compared with a simulation involving 10^4 particles placed in 28 bins.

$f(\dot{z}_f)$ as a smooth line in Figure 3a; the function rises linearly at small $\dot{z}_f$, peaks at $\dot{z}_f \approx 1.44(E_0/a)^{1/2}$, and falls exponentially at large $\dot{z}_f$. The histogram in Figure 3a was obtained from a numerical simulation by binning the final parallel particle velocities.

The distribution function can also be written in terms of the parallel energy: $F(\mathcal{E}_\parallel) = f(\dot{z}_f)d\dot{z}_f/d\mathcal{E}_\parallel$, where $\mathcal{E}_\parallel = \dot{z}_f^2/2$. Furthermore, this function can be integrated to obtain $N(\mathcal{E}_\parallel)$, the number of particles with energy greater than $\mathcal{E}_\parallel$:

$$N(\mathcal{E}_\parallel) \equiv \int_{\mathcal{E}_\parallel}^{\infty} d\mathcal{E}_\parallel F(\mathcal{E}_\parallel) = N_{\text{tot}}\frac{1 - \exp\left(-a\mathcal{E}_\parallel/E_0\right)}{\sinh\left(a\mathcal{E}_\parallel/E_0\right)}. \quad (11)$$

We plot the exponential tail,

$$N(\mathcal{E}_\parallel) \sim 2N_{\text{tot}}\exp(-a\mathcal{E}_\parallel/E_0),$$

in Figure 3b. The histogram in Figure 3b was obtained from a numerical simulation by binning the final parallel

particle energies. Because of statistical problems associated with binning a finite number of particles, it is more convenient to plot $N(\mathcal{E}_\parallel)$ rather than $F(\mathcal{E}_\parallel)$.

Comparison with Previous Work

Previous workers have studied test particle motion near a magnetic x line in the limit $B_\parallel = 0$ [*Bulanov and Syrovatskii*, 1976] and used those results to obtain an energy spectrum much as we did above [*Bulanov and Sasarov*, 1976]. Their magnetic field is identical to the x-y projection of our magnetic field, and their $E_\parallel$ has the same form as ours, with $\mu \sim 1$. These previous results were obtained asymptotically in the limit of large $\mathcal{E}_\parallel$, so only the high-energy tail of the distribution was found.

We present in equation 12a the function $F_{BS}(\mathcal{E}_\parallel)$ obtained by Bulanov and Sasarov for the nonrelativistic limit [*Bulanov and Sasorov*, 1976, equation (25)], converting their notation to ours. For comparison, we present the asymptotic form of our $F(\mathcal{E}_\parallel)$ in equation 12b, having restored physical units:

$$F_{BS}(\mathcal{E}_\parallel) \sim A\frac{a}{DeE_\parallel}N_{tot} \cdot \exp\left(-k^{3/4}\frac{\left(ma^2D^2\Omega_0^2\right)^{1/4}}{DeE_\parallel}\mathcal{E}_\parallel^{3/4}\right); \quad (12a)$$

$$F(\mathcal{E}_\parallel) \sim 2\frac{a\epsilon}{DeE_\parallel}N_{tot}\exp\left(-\frac{a\epsilon}{DeE_\parallel}\mathcal{E}_\parallel\right). \quad (12b)$$

The constants A and k are unknown quantities of order unity. $F_{BS}(\mathcal{E}_\parallel)$ yields a slightly harder energy spectrum than does our $F(\mathcal{E}_\parallel)$, because it has $\mathcal{E}_\parallel$ raised to the 3/4 power. More important, the characteristic energy associated with the two exponentials scale differently with the physical parameters in the problem: Bulanov and Sasarov obtain a characteristic energy (i.e., decay constant) $\mathcal{E}_{\parallel BS} = kD^{2/3}(eE_\parallel)^{4/3}(ma^2\Omega_0^2)^{-1/3}$, whereas we obtain $\mathcal{E}_\parallel = DeE_\parallel/a\epsilon$.

We have seen above that the characteristic energy of accelerated particles is determined by the amount of time a typical particle spends near the reconnection region (or box). This time is given approximately for our problem by equation (5). If we set $\Omega_\parallel = 0$ in equations 2a and 2b, we recover the Bulanov and Sasorov problem and can solve for the particle motion analytically if we assume $\dot{z} \approx eE_\parallel t/m$. (This is only valid for particles very close to the x line, where $E_\parallel$ dominates the dynamics and chaotic effects are not important.) Considering the limit of large t leads to a characteristic energy which agrees with equation 12a.

Friedman [1969] presented a numerical study of particle trajectories in a Petschek field configuration, which is very similar to our model field in the absence of $B_\parallel$. The electric field used by Friedman is $E_\parallel = av_{A0}B_0/c$ (with $a = 0.1$), which is of the same form as that used by Bulanov and Sasorov and by us (with $\mu = a$). The simulation involved 100 test particles (ions) distributed randomly around the x line with a thermal velocity distribution. In Figure 4 of Friedman's paper, $N(\mathcal{E})$ vs. $\mathcal{E}$ is plotted, where $\mathcal{E}$ is the total particle energy and $N(\mathcal{E})$ is found to have an exponential tail with a characteristic energy $\mathcal{E}_F$, which can be found graphically.

In Table 3, we present a comparison of $\mathcal{E}_0, \mathcal{E}_{BS}$, and (where applicable) $\mathcal{E}_F$ for two very different choices of values for the physical parameters. In each case, we show the results for both electrons and protons, and we also give the resulting values of E_0 and r_g. The parameter values chosen for the first row are taken from *Friedman* [1969], and those of the second row are taken from *Syrovatskii* [1966]. These comparisons are somewhat awkward, because the addition of $B_\parallel$ fundamentally alters the geometry of the problem. We proceed simply by letting the characteristic magnetic field equal $B_\parallel$ when calculating $\mathcal{E}_0$, then letting it equal B_0 when calculating $\mathcal{E}_{B\&S}$ and $\mathcal{E}_F$. Table 3 shows that $\mathcal{E}_\parallel$ and $\mathcal{E}_{B\&S}$ are comparable for ions, whereas $\mathcal{E}_0$ can be orders of magnitude larger than $\mathcal{E}_{B\&S}$ for electrons. The acceleration time $t_{stream} \sim t_{stream}/\Omega_\parallel$, which is given in the last column of Table 3, is seen to be extremely short compared with the risetime for solar flare hard X ray emission [*Forman et al.*, 1986]. If we identify the latter time scale with the rate of evolution of the electromagnetic fields, the static approximation we have made for the fields appears to be justified.

Conclusion

We present the first study of test-particle acceleration near a magnetic x line in which a strong component of the magnetic field along the x line is assumed. Comparison with similar studies in which there was no parallel magnetic field component shows that the addition of this component can result in a characteristic energy of accelerated particles which scales very differently with the physical parameters in the problem.

The exponential spectrum given by equation 12b is in reasonably good agreement with energetic proton spectra observed in space and inferred from gamma ray

TABLE 3. Two Specific Cases for Comparison ($\mu = a = \epsilon = 0.1$)

Particle	E_0	r_g	$\mathcal{E}_0$, eV	$k^{-1}\mathcal{E}_{BS}$, eV	$\mathcal{E}_F$, eV	t_{stream}, s
Case 1						
ions	2×10^{-2}	8×10^{-2}	2×10^3	7×10^3	7×10^4	4×10^{-5}
electrons	1×10^{-5}	2×10^{-3}	2×10^3	600	...	1×10^{-6}
Case 2						
ions	3×10^{-6}	8×10^{-6}	3×10^7	5×10^6	...	2×10^{-2}
electrons	1.5×10^{-6}	2×10^{-7}	3×10^7	4×10^5	...	4×10^{-4}

Case 1: $B_\parallel = 500$ G, $n = 2 \times 10^{11}$ cm^{-3}, $D = 20$ cm, $k_BT = 100$ eV. Case 2: $B_\parallel = 100$ G, $n = 5 \times 10^9$ cm^{-3}, $D = 1 \times 10^6$ cm, $k_BT = 100$ eV.

observations [*Forman et al.*, 1986], and the characteristic energy of tens of MeV is similar to that required by the data. In view of the simple model we have used and our complete neglect of propagation effects in the loop, this agreement may be fortuitous. Furthermore, we have treated the particles as test particles. If the acceleration mechanism is efficient, the feedback of the particles on the fields must be included self-consistently.

Acknowledgments. We are happy to acknowledge support by NSF grant ATM-9012517 to the Universiy of Colorado.

The Editor thanks two referees for their assistance in evaluating this paper.

REFERENCES

Bender, C. M. and S. A. Orszag, *Advanced Mathematical Methods for Scientists and Engineers*, pp. 544–568, chap. 11, McGraw-Hill, New York, 1978.

Bulanov, S. V. and P. V. Sasorov, Energy spectrum of particles accelerated in the neighborhood of a line of zero magnetic field, *Sov. Astron.*, Engl. Transl., *19*, 464–468, 1976.

Bulanov, S. V., and S. I. Syrovatskii, Motion of charged particles in the vicinity of the zero line of a magnetic field, *Proc. Lebedev Phys. Inst.*, *88*, 109–120, 1976.

Burkhart, G. R., J. F. Drake, and J. Chen, Magnetic reconnection in collisionless plasmas: Prescribed fields, *J. Geophys. Res.*, *95*, 18,833–18,848, 1990.

Channell, P. J., and C. Scovel, Symplectic integration of Hamiltonian systems, *Nonlinearity*, *3*, 231–259, 1990.

Chiueh, T., and E. G. Zweibel, The structure and dissipation of forced current sheets in the solar atmosphere, *Astrophys. J.*, *317*, 900–917, 1987.

Forman, M. A., R. Ramaty, and E. G. Zweibel, The acceleration and propagation of solar flare energetic particles, in *Physics of the Sun*, vol. II, chap. 13, edited by P. A. Sturrock, pp. 249–289, D. Reidel, Hingham, Mass., 1986.

Friedman, M., Possible mechanism for the acceleration of ions in some astrophysical phenomena, *Phys. Rev.*, *182*, 1408–1414, 1969.

Martin, R. F., Jr., Chaotic particle dynamics near a two-dimensional magnetic neutral point with application to the geomagnetic tail, *J. Geophys. Res.*, *91*, 11,985–11,992, 1986.

Nicholson, D. R., in *Introduction to Plasma Theory*, pp. 17–23, chap 2., John Wiley, New York, 1983.

Parker, E. N., Sweet's mechanism for merging magnetic fields in conducting fluids, *J. Geophys. Res.*, *62*, 509–520, 1957.

Petschek, H. E., Magnetic field annihilation, AAS-NASA Symposium on the Physics of Solar Flares, *NASA Spec. Publ.*, *SP-50*, 425–439, 1964.

Sturrock, P. A. (Ed.), Flare models, in *Solar Flares*, pp. 411–449, chap. 9, Colorado Associated University Press, Boulder, 1980.

Sweet, P. A., The neutral point theory of solar flares, in *Electromagnetic Phenomena in Cosmical Physics*, edited by B. Lehnert, pp. 123–134, Cambridge University Press, New York, 1958.

Syrovatskii, S.I., Dynamic dissipation of a magnetic field and particle acceleration, *Sov. Astron.*, Engl. transl., *10*, 270–280, 1966.

Van Hoven, G., Solar flares and plasma instabilities: Observations, mechanisms and experiments, *Sol. Phys.*, *49*, 95–116, 1976.

D. L. Bruhwiler, Grumman Space Systems, 4 Independence Way, Princeton, NJ 08540.

E. G. Zweibel, Department of Astrophysical, Planetary, and Atmospheric Sciences, University of Colorado, Boulder, CO 80309.

(Received February 18, 1992;
accepted March 6, 1992.)